Study and evaluation of the damage performance of a 120-mm multi-effect warhead using numerical simulation

Nguyen Dinh Linh*, Le Tuan Anh, Nguyen Hoa Binh,
Le Hai Thuong, Nguyen The Duy, Tran Van De

Institute of Missile, Academy of Military Science and Technology, 17 Hoang Sam, Nghia Do, Hanoi, Vietnam.
*Corresponding author: dinhlinhk20@gmail.com
Received 19 Jun. 2026; Revised 14 Aug. 2026; Accepted 04 Sep. 2026; Published 16 Sep. 2026.
DOI: https://doi.org/10.54939/1859-1043.j.mst.FMC.2026.98-107

ABSTRACT

This paper presents a methodology for studying and evaluating the damage performance of a 120-mm multi-effect warhead by combining analytical calculations and numerical simulations using ANSYS Autodyn 2D/3D. The study focuses on analysing the formation process of the shaped charge jet and the dispersion characteristics of fragments through the application of the JWL equation of state for high explosives and the Johnson-Cook strength model coupled with the Shock EOS for metallic components. This approach is used to evaluate the combined effectiveness of shaped-charge penetration and fragmentation within a single warhead structure, thereby predicting its damage capability against various battlefield targets. The obtained results play an important role in optimizing design parameters and contribute to improving the effectiveness of damage performance assessment for new-generation ammunition systems, while significantly reducing the cost and time required for full-scale experimental testing.

Keywords: Multi-effect warhead; Shaped charge jet; Fragmentation; Johnson-Cook model.

1. INTRODUCTION

A multi-effect warhead is a type of warhead capable of defeating various types of targets or functioning through different mechanisms to meet specific combat requirements. Worldwide, this type of warhead has been widely studied and applied, with typical examples including the Geran-1 [8], S8KO, and S8KOM warheads [9].

Previous studies have effectively addressed the problems of describing warhead geometry, the formation mechanism of the shaped charge jet, and the fragment dispersion process. However, most traditional analytical models [2] usually simplify the problem by neglecting complex changes in the physical state of materials, which may lead to significant calculation errors. Therefore, when these formulae are used, appropriate empirical coefficients must be selected, and the calculated results are only approximate. At present, the problem of evaluating the damage performance of multi-effect warheads has not been satisfactorily resolved. Domestic studies have mainly focused on separately investigating the shaped-charge penetration effect of shaped charge warheads [3, 6, 7, 10] or the fragment dispersion law of metallic casings under the action of detonation waves [1, 5, 11, 13]. Such an approach does not accurately reflect the simultaneous effects occurring within the same warhead structure, thereby imposing considerable limitations on damage performance assessment. Moreover, experimental methods require substantial investment costs, long testing durations, and face difficulties in collecting intermediate parameters under actual detonation conditions.

With the development of science and technology, numerical simulation enables a clearer understanding of the complex nature of each ammunition terminal-effect process. In addition, simulation allows relatively comprehensive visualization of relevant parameters and makes it possible to investigate the influence of multiple parameters on ammunition effects, which is difficult to achieve using other methods. At present, the terminal effects of ammunition can be simulated using various approaches, including commercial software packages such as ANSYS LS-

DYNA, ANSYS AUTODYN, and ABAQUS. Initially, numerical simulation was mainly based on the finite element method (FEM). However, for problems involving large deformation, high velocity, and local failure, such as ammunition terminal-effect problems, continuous remeshing is often required during the simulation process, which increases computational time and may lead to numerical errors. In contrast, the Eulerian mesh coupled with the Lagrangian mesh can overcome these limitations.

In this paper, the authors propose a combined analytical and numerical simulation approach to evaluate the damage performance of a multi-effect warhead. Specifically, the damage performance of a 120-mm warhead is evaluated to comprehensively analyze the formation process of the shaped charge jet based on the JWL equation of state for high explosives, while simultaneously assessing the fragment dispersion characteristics using the Johnson-Cook strength model coupled with the Shock EOS for metallic components.

2. METHODOLOGY FOR EVALUATING THE LETHALITY OF MULTI-PURPOSE WARHEADS

2.1. Fragmentation effect

Determining the impact velocity of fragments is highly complicated, since the motion of fragments in air depends strongly on their mass, velocity, shape, and other related factors, while accurately determining these parameters is extremely difficult.

To solve this problem, the following assumptions are introduced:

- The influence of the fragment weight on the flight trajectory is neglected; therefore, the fragment trajectory is assumed to be a straight line.

- Upon impacting the target, the fragment still retains sufficient energy to defeat the target.

The impact velocity of a fragment is defined as the velocity of the fragment at the moment it reaches the target. During flight, the fragment velocity decreases according to the following law [2]:

$$m_0 \frac{dv}{dt} = -R \tag{1}$$

where:

The air resistance acting on the fragment is given by

$$R = C_x.S_0.\rho.\frac{v^2}{2} \tag{2}$$

ρ - Air density; (ρ=1,293 kg/m^3)

C_x - Coefficient of frontal air resistance

The value of C_x depends on the fragment velocity. The relationship $C_x = f(v)$ is expressed as follows [2]:

$$c_x = \begin{cases} 0,5 & \text{for } v \le 150 m/s \\ \left[(1,49 + 0,51\sin(860^o - 360^o \lg v)\right]^{-1} & \text{for } 150 < v \le 550 m/s; \\ 0,855\left(1 + \dfrac{50}{v}\right) & \text{for } v > 550 m/s \end{cases}$$

where: S_0: Midsectional area of the fragment

The fragment mass and its average cross-sectional area are related by the following expression:

$$S_0 = \Phi.\left(\frac{m}{\rho_m}\right)^{\frac{2}{3}}; \tag{3}$$

where: Φ - fragment shape factor; ρ_m – density of the fragment material;

Equation (1) can be rewritten as:

$$m_0 \frac{dv}{dt} = -C_x.S_0.\rho.\frac{v^2}{2} \text{ on the other hand } \quad \frac{dv}{dt} = \frac{dv}{dx}\frac{dx}{dt} = v\frac{dv}{dx}$$

Substituting into Eqquation (1), we obtain

$$m_0 \frac{dv}{dx} = -C_x.S_0.\rho.\frac{v}{2} \Leftrightarrow \quad \frac{dv}{v} = -\frac{C_x.S_0.\rho}{2m_0}dx$$

Integrating both sides with the velocity varying from v_{bt} to v_{vc}, and the travel distance varying from 0 to x_{mt}

$$\int_{vbt}^{v_{vc}} \frac{dv}{v} = -\frac{C_x S_0.\rho}{2m_0}\int_0^{x_{mt}} dx \Leftrightarrow \ln\frac{v_{vc}}{v_{bt}} = -\frac{C_x S_0.\rho}{2m_0}x_{mt} \Rightarrow v_{vc} = v_{bt}\exp\left(-\frac{C_x S_0 \rho.x_{mt}}{2m_0}\right) \tag{4}$$

The lethal energy of a fragment is an important parameter for assessing its lethality, as it directly affects the probability of target defeat.

At present, the lethality of a fragment is commonly evaluated based on its specific kinetic energy, defined as the kinetic energy of the fragment per unit area of its average cross section:

$$E_r = \frac{m_0 v_{vc}^2}{2S_{tb}} \tag{5}$$

where: E_r - specific energy of the fragment upon target impact; v_{vc} - fragment velocity upon target impact; m_0 - fragment mass; S_{tb} - average cross-sectional area of the fragment.

Thus, it is necessary to determine the relationship between E_r and the target-defeat probability of the fragment. In addition to the fragment energy, this relationship also depends on the target characteristics. For simplicity, a stepwise kill criterion is used to define this relationship. The minimum energy required for a fragment to defeat the target ($E_{r.\min}$) is assumed to be known.

According to the stepwise kill criterion:

where $E_r > E_{r.\min}$, the target-defeat probability is $P_{td} = 1$;

where $E_r < E_{r.\min}$, the target-defeat probability is $P_{td} = 0$

Thus, all fragments are divided into two groups: effective and ineffective fragments, corresponding to kill and no-kill outcomes. The number of effective fragments can be determined according to the following condition:

$$E_r > E_{r.\min}$$

Substituting Equations (4) and (5) into the above condition gives:

$$\frac{m_0 v_{vc}^2}{2S_{tb}} \geq E_{r.\min} \quad \Rightarrow \frac{m_0}{2S_{tb}}\left[v_0 \exp\left(-\frac{C_x S_0 \rho x_{mt}}{2m_0}\right)\right]^2 \geq E_{r.\min} \tag{6}$$

If the mass of a lethal fragment and its average cross-sectional area are related by the following expression [2]:

$$S_{tb} = k_{hd}.m_0^{2/3} \tag{7}$$

where: k_{hd} - fragment shape coefficient. For steel-cased ammunition ($k_{hd} = 0,005 m^2 / kg^{2/3}$)

Substituting Equation (7) into Equation (6), the maximum distance at which the fragment can still defeat the target is determined as:

$$\frac{m_0^{1/3}}{2.k_{hd}}\left[V_o.\exp(-\frac{C_x.k_{hd}.\rho.x_{mt}}{2.m_0^{1/3}})\right]^2 \geq E_{r.\min} \tag{8}$$

where: m_0 - fragment mass; k_{hd} - fragment shape coefficient; V_0 - initial fragment velocity; C_x - coefficient of frontal air resistance; ρ - air density; x_{mt} - distance from the explosion center to the target; $E_{r.\min}$ - minimum specific lethal energy required to defeat the target.

2.2. Shaped-charge penetration effect

According to previous studies [3, 6, 7, 10], the simulation of jet formation and its penetration into a steel plate can be decoupled into two separate sub-problems: the jet formation process and the subsequent penetration process. The jet parameters analyzed in the formation stage serve as the input data for the penetration stage. The explosive wave propagation and jet formation are modeled using an Eulerian mesh, whereas the target penetration process utilizes a Lagrangian mesh. To evaluate grid sensitivity, both the jet and the target were meshed using three different cell sizes: 0.25 × 0.25 mm, 0.5 × 0.5 mm, and 1 × 1 cm. Ultimately, to minimize the total element count, reduce computational time, and ensure solution convergence, a mesh size of 0.5 × 0.5 mm was selected for both the jet and the target (Figure 1).

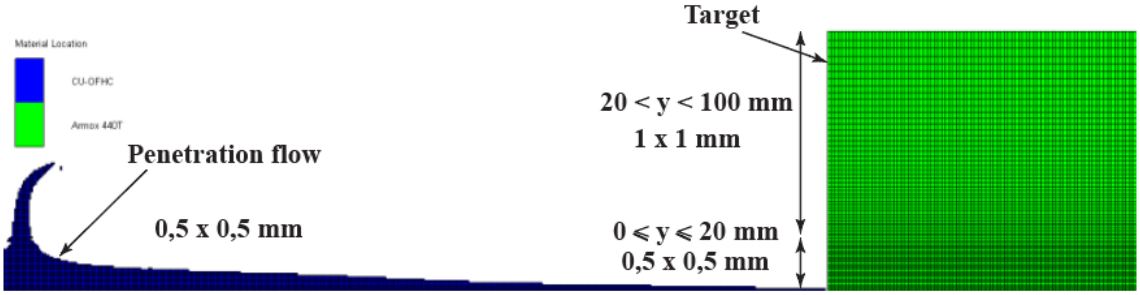


Figure 1. *Mesh of the simulation model for the jet impact and penetration process.*

The material properties and their corresponding equations of state used in the simulation are presented in the tables below:

The A-IX-1 explosive and the PEN1.77 detonating explosive are described using the JWL equation of state [3, 4]. The JWL equation-of-state parameters of A-IX-1 are given in Table 1.

The liner material is Cu-OFHC, which exhibits good ductility; however, under impact loading and high strain-rate deformation, it is described using the Shock equation of state and the Steinberg-Guinan strength model. The Shock EOS parameters and Steinberg-Guinan strength-model parameters are taken from the software library [4] and are listed in Tables 2 and 3.

Table 1. *JWL equation-of-state parameters of the explosives.*

A-IX-I explosive							
ρ_0 *(kg.m^{-3})*	A *(MPa)*	B *(MPa)*	R_1	R_2	ω	E_0 *(kJ.m^{-3})*	D *(m.s^{-1})*
1700	5,37167e5	5,37926e3	4,2	1	0,4	1,36e7	7500
PEN1.77 explosive							
1,77	6,17e5	1,69e4	4,4	1,2	0,25	1,01e7	8300

Table 2. *Shock EOS parameters of the Cu-OFHC liner.*

ρ_0 *(g.cm^{-3})*	Γ	C_1 *(m.s^{-1})*	S_1	C_2 *(cm.μs^{-1})*	S_2	$\frac{VE}{v_0}$	$\frac{VB}{v_0}$
8,96	*2,02*	*3940*	*1,489*	*0*	*0*	*0*	*0*

Table 3. *Steinberg-Guinan strength-model parameters of the liner.*

G *(MPa)*	σ_c^0 *(MPa)*	$\sigma_{c\max}^d$ *(Mpa)*	β	n	G_p'	G_T' *(kPa/K)*	$(\sigma_c^d)_p'$	T_{nc} *(K)*
4,47e4	*1,2e2*	*6,4e2*	*36*	*0,45*	*1,35*	*-1,798e4*	*0,0034*	*1790*

The casing materials are STEEL 4340 and AL7039. Under explosive loading, these materials undergo large deformation accompanied by changes in both volume and shape; therefore, the Shock equation of state and the Johnson-Cook strength model are used. The Shock EOS parameters and Johnson-Cook strength-model parameters are taken from the software library [4] and are listed in Tables 4, 5, and 6.

Table 4. *Shock EOS parameters of the AL7039 casing.*

ρ_0 *(g.cm^{-3})*	Γ	C_1 *(m.s^{-1})*	S_1	C_2 *(cm.μs^{-1})*	S_2	$\frac{VE}{v_0}$	$\frac{VB}{v_0}$
2,77	2	5,328e3	1,338	0	0	0	0

Table 5. *Johnson-Cook strength-model parameters of the AL7039 casing.*

ρ_0 *(g.cm^{-3})*	A *(MPa)*	B *(MPa)*	C	n	m	T_{room} *(K)*	T_{nc} *(K)*
2,77	3,37e2	3,43e2	0,01	0,41	1	300	877

Table 6. *Johnson-Cook strength-model parameters of the outer STEEL 4340 casing.*

ρ_0 *(g.cm^{3})*	A *(MPa)*	B *(MPa)*	C	n	m	T_m *(K)*
7,830	792	510	0,014	0,26	1,03	1793

The wave shaper material used in the simulation of the shaped-charge jet formation process is Plexiglass. The material behavior is described using the Shock equation of state.

The Shock EOS parameters of Plexiglass are taken from the software library [4] and are listed in Table 7.

Table 7. *Shock EOS parameters of the Plexiglass.*

ρ_0 *(g.cm^{-3})*	Γ	C_1 *(m.s^{-1})*	S_1	C_2 *(cm.μs^{-1})*	S_2	$\frac{VE}{v_0}$	$\frac{VB}{v_0}$
1,186	0,97	2,598e3	1,516	0	0	0	0

Based on the equivalence of steel grades according to relevant standards, Armox 440T is selected as the target material in the simulation [3]. The Johnson-Cook strength-model parameters and failure-model parameters are listed in Tables 8 and 9.

Table 8. *Johnson-Cook strength-model parameters of the target.*

ρ_0 $(g.cm^{-3})$	A (MPa)	B (MPa)	C	n	m	T_{room} (K)	T_{nc} (K)
7,896	1,11e3	2e3	0,002	0,85	1,4	300	1793

Table 9. *Johnson-Cook failure-model parameters.*

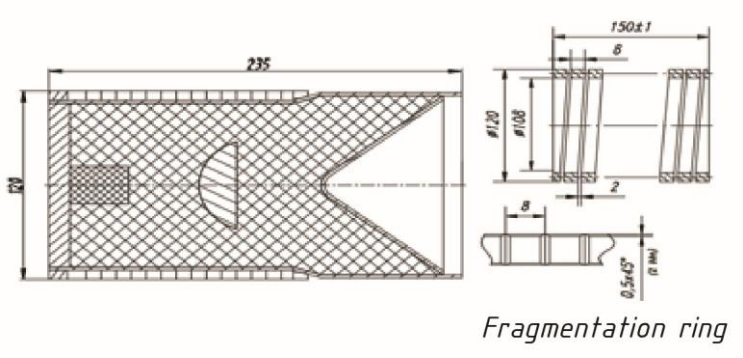
D_1	D_2	D_3	D_4	D_5
0,051	0,82	-0,46	-0,04	0

3. RESULTS OF DAMAGE PERFORMANCE EVALUATION OF THE 120-MM MULTI-EFFECT WARHEAD USING AUTODYN

3.1. Geometric model

The warhead has a cylindrical configuration with a length of 235 mm and a diameter of 120 mm. To provide the fragmentation effect, the warhead consists of an aluminium cylindrical casing filled with A-IX-1 explosive. The cylindrical casing is wound with 15 turns of steel wire pre-cut with stress grooves, with each turn consisting of 47 preformed fragments measuring 8 × 8 × 6 mm, giving a total of 705 fragments (Figure 2a). To provide the shaped-charge penetration effect, a 2-mm-thick copper liner is arranged at the front of the warhead, together with a synthetic-plastic wave shaper (Figure 2b). Thus, upon detonation, the warhead simultaneously produces shaped-charge penetration and fragmentation effects.

a. Model of the fragmentation section



b. Model of the shaped-charge section

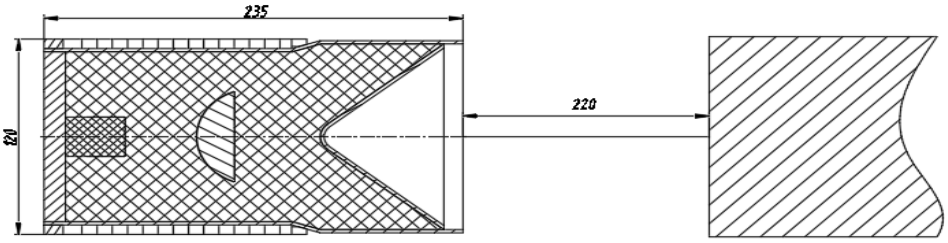
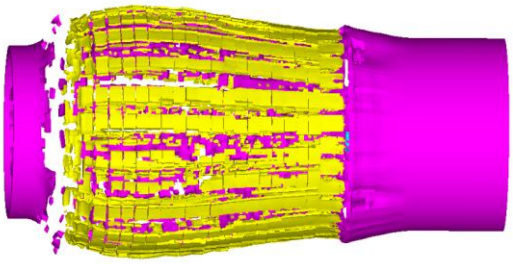


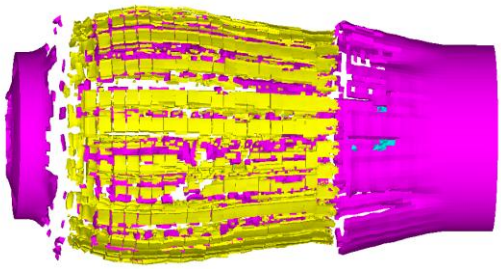
Figure 2. *Warhead models classified by damage effect.*

3.2. Simulation results using ANSYS autodyn

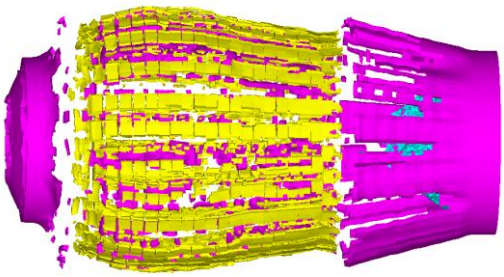
3.2.1. Fragmentation effect



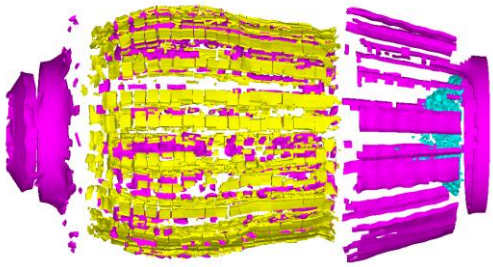
a. Fragmentation results at 16 μs;



b. Fragmentation results at 23 μs;



c. Fragmentation results at 32 μs;



d. Fragmentation results at 50,7 μs.

Figure 3. *Fragmentation simulation results at different time instants.*

Table 10. *Fragment-field parameters.*

Fragment Number	Elements in Fragment	Mass	Center-X	Center-Y	Center-Z	Volume	Average Speed
13	192	2,59E+06	-43,57	-55,92	21,34	3,30E+05	793
17	798	2,05E+06	10,60	45,75	35,30	2,61E+05	1.290
18	844	1,99E+06	45,13	46,19	-15,08	2,54E+05	1.365
20	176	1,82E+06	-48,67	10,91	-46,53	2,32E+05	1.260
…	…	…	…	…	…	…	…
708	7	1,64E+05	8,57	-4,15	-73,25	2,10E+04	1.528
709	9	1,64E+05	-69,99	-35,55	-18,20	2,10E+04	1.377

Based on the fragment-field parameters obtained from Table 10, the average fragment velocity is determined to be approximately $v_{bt} \approx 1383$ m/s. The analytical method is then used to evaluate the fragmentation damage performance of the warhead.

$m_0 = 3g$ - Fragment mass; $k_{hd} = 0,005 m^2 / kg^{2/3}$ - Fragment shape coefficient (for steel fragments) [2]; $V_0 = v_{bt} = 1383 m/s$ - Initial fragment velocity; Coefficient of frontal air resistance $C_x = 0,855.(1 + \frac{50}{v}) = 0,908$, since $v_{bt} > 550 m/s$; $\rho = 1,293 kg/m^3$ - Air density; x_{mt} - Distance from the explosion center to the target; $E_{r.\min}$ - Minimum specific lethal energy required to defeat the target. For a conventional target, with $E_{r.\min} = 13,2.10^6 J/m^2$ [2], Equation (8) is satisfied when

$x_{mt} \leq 18{,}11m$. Therefore, the lethal radius of the warhead is: $R_{st} = 18{,}11\ m$

3.2.2. Shaped-charge penetration effect

The simulation results allow the variation in the axial velocity of the jet to be determined. For a shaped charge jet with a large axial velocity gradient, the jet elongation capability increases. This is a factor that enhances penetration capability. However, if the jet has a large axial velocity gradient while its diameter is small, jet breakup may occur. This, in turn, reduces the penetration depth of the shaped charge (Figure 4).

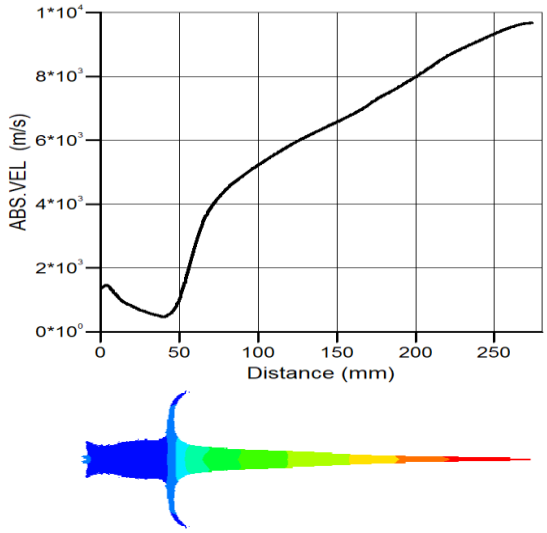
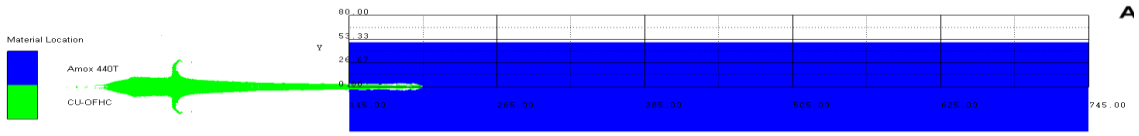
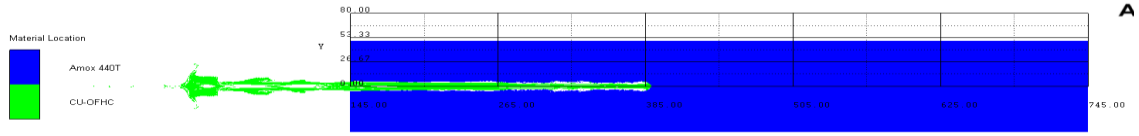


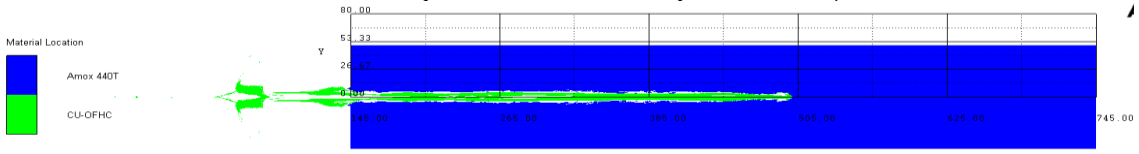
Figure 4. *Axial velocity distribution of the jet at 53,2 μs.*



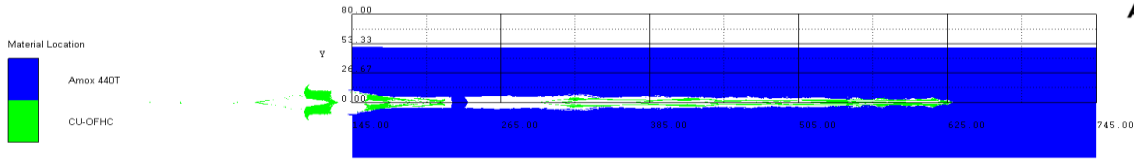
a. Penetration process into the steel plate at 45,2 μs;



b. Penetration process into the steel plate at 93,6 μs;



c. Penetration process into the steel plate at 137,5 μs;



d. Penetration process into the steel plate at 225 μs.

Figure 5. *Penetration process into the steel plate.*

The simulation results are shown in Figure 5. The formed shaped charge jet reaches a maximum velocity of nearly 9816 m/s and penetrates a 480-mm-thick steel plate after 225 μs. This damage performance is sufficient to defeat targets such as lightly armoured vehicles and infantry fighting vehicles.

4. CONCLUSIONS

This paper develops a numerical model to evaluate the simultaneous lethality (shaped charge penetration and fragmentation) of a 120-mm multi-purpose warhead utilized for short-range coastal defense missiles. By closely integrating analytical theoretical calculations with highly non-linear dynamic simulations in the ANSYS Autodyn environment, the study has achieved several key results as follows:

Regarding the fragmentation field formation mechanism: The fracture process of the STEEL4340 alloy casing under the loading of detonation waves from the A-IX-I high explosive was successfully simulated. The resulting fragment field achieved an average velocity of approximately V_o = *1383 m/s*. The effective lethal radius against personnel was determined to be $R_{st} = 18{,}11m$, ensuring optimal fragment density and energy to suppress wide-area, thin-skinned targets, such as landing craft air cushions (LCACs) and high-speed boats.

Regarding the shaped charge jet penetration effect: The formation process of the shaped charge jet reached a peak velocity of approximately ≈ 9816 *m/s*, demonstrating the capability to penetrate an Armox 440T steel target plate with a thickness of 480 *mm*. This lethal performance is fully sufficient to defeat heavily armored targets, such as enemy main battle tanks or amphibious armored vehicles.

The reliability of the numerical simulation method was validated by benchmarking against experimental data of the S8KOM rocket warhead, with the resulting error not exceeding 15%.

REFERENCES

[1]. Held, M., *"Fragmentation warheads"*, Journal of Energetic Materials, Vol. 22, No. 3, pp. 181-203, (2004).

[2]. Nguyễn Văn Thuỷ, Trần Văn Định, *"Uy lực đạn"*, Học viện Kỹ thuật Quân sự, Hà Nội, (2007) (in Vietnamese).

[3]. T. Sy Ngo, S. Beer and P. Konečný*, *"Effect of Target Arrangement and Target Materials Properties on Penetration Depth"*, Advances in Military Technology, Vol. 15, No. 2, pp. 436-449, (2020).

[4]. ANSYS Autodyn User's Manual, http://www.ansys.com, (2021).

[5]. Nguyễn Quốc Anh, *"Nghiên cứu ảnh hưởng của một số yếu tố đến hiệu quả tạo mảnh của đầu đạn sát thương có rãnh tập trung ứng suất"*, Luận án Tiến sĩ Kỹ thuật, (2017) (in Vietnamese).

[6]. Nguyễn Đình Linh, Lê Hải Thượng, Nguyễn Xuân Thành, *"Tối ưu các tham số kết cấu phần chiến đấu đến khả năng xuyên của đầu nổ lõm"*, Tạp chí nghiên cứu khoa học và công nghệ, Số đặc san FEE, No. 12, pp. 212-218, (2024) (in Vietnamese).

[7]. Nguyễn Đình Linh, Phạm Đình Trưởng, Nguyễn Như Quế, *"Xác định tiêu cự nổ của đầu đạn tên lửa 125mm bằng phương pháp mô phỏng"*, Hội nghị các nhà khoa học nghiên cứu trẻ lần thứ XVIII – Năm 2023, (2023) (in Vietnamese).

[8]. Conflict Armament Research, *"Dissecting Iranian drones employed by Russia in Ukraine"*, https://conflictarm.org/Iraniandronewarheads, (2022).

[9]. S-8KOM Aviation unguided rocket, https://www.yugoimport.com/sites/default/files/documents/2022-09/80%20mm%20S-8%20KOM.pdf.

[10]. Phạm Hữu Nguyên, *"Nghiên cứu ảnh hưởng của tấm chắn sóng nổ đến chiều sâu xuyên đạn lõm"*, Luận án Tiến sĩ Kỹ thuật, (2021) (in Vietnamese).

[11]. Nguyễn Quốc Anh, Trần Đình Thành, *"Nghiên cứu ảnh hưởng của rãnh ứng suất đến đặc tính sinh mảnh của đầu đạn sát thương"*, Hội nghị KH&CN toàn quốc về Cơ khí - Động lực 2016, tập 2, (2016) (in Vietnamese).

[12]. Moxnes, J. F., Prytz, A. K., Frøyland, Ø., Klokkehaug, S., Skriudalen, S., Friis, E., ... & Ødegårdstuen, *"Experimental and numerical study of the fragmentation of expanding warhead casings by using different numerical codes and solution techniques"*, Defence technology, (2014).
[13]. Hoàng Văn Cường, Nguyễn Quốc Anh, *"Mô phỏng số trường mảnh đạn sát thương"*, Tạp chí Khoa học & Kỹ thuật, (2015) (in Vietnamese).

TÓM TẮT

Nghiên cứu, đánh giá uy lực của đầu nổ đa tác dụng cỡ 120mm bằng phương pháp mô phỏng

Bài báo trình bày phương pháp nghiên cứu và đánh giá uy lực của đầu nổ đa tác dụng cỡ 120mm thông qua sự kết hợp giữa tính toán giải tích và mô phỏng số trên môi trường ANSYS Autodyn 2D/3D. Nghiên cứu tập trung phân tích quá trình hình thành dòng xuyên lõm và đặc tính phân tán mảnh văng thông qua việc ứng dụng phương trình trạng thái JWL cho thuốc nổ mạnh và mô hình bền Johnson-Cook kết hợp với Shock EOS cho các thành phần kim loại để đánh giá hiệu quả tổng hợp uy lực xuyên lõm và phân mảnh trong cùng một cấu trúc đầu nổ, từ đó dự báo khả năng tiêu diệt các loại mục tiêu đa dạng trên chiến trường. Kết quả nghiên cứu đóng vai trò quan trọng trong việc tối ưu hóa các tham số thiết kế mà còn góp phần vào việc nâng cao hiệu quả đánh giá uy lực các hệ thống đạn dược thế hệ mới, giúp giảm thiểu đáng kể chi phí và thời gian thử nghiệm thực tế.

Từ khoá: Đầu nổ đa tác dụng; Dòng xuyên lõm; Nổ phân mảnh; Mô hình Johnson-Cook.